

RESEARCH

Open Access



Aberrant oscillatory activity in neurofibromatosis type 1: an EEG study of resting state and working memory

Samantha J. Booth¹, Shruti Garg^{2,3}, Laura J. E. Brown², Jonathan Green^{2,3}, Gorana Pobric¹ and Jason R. Taylor^{1*} 

Abstract

Background Neurofibromatosis type 1 (NF1) is a genetic neurodevelopmental disorder commonly associated with impaired cognitive function. Despite the well-explored functional roles of neural oscillations in neurotypical populations, only a limited number of studies have investigated oscillatory activity in the NF1 population.

Methods We compared oscillatory spectral power and theta phase coherence in a paediatric sample with NF1 ($N=16$; mean age: 13.03 years; female: $n=7$) to an age/sex-matched typically developing control group ($N=16$; mean age: 13.34 years; female: $n=7$) using electroencephalography measured during rest and during working memory task performance.

Results Relative to typically developing children, the NF1 group displayed higher resting state slow wave power and a lower peak alpha frequency. Moreover, higher theta power and frontoparietal theta phase coherence were observed in the NF1 group during working memory task performance, but these differences disappeared when controlling for baseline (resting state) activity.

Conclusions Overall, results suggest that NF1 is characterised by aberrant resting state oscillatory activity that may contribute towards the cognitive impairments experienced in this population.

Trial registration ClinicalTrials.gov, NCT03310996 (first posted: October 16, 2017).

Keywords Electroencephalography (EEG), Neurofibromatosis type 1 (NF1), Oscillations, Oscillatory power, Phase coherence, Working memory

*Correspondence:

Jason R. Taylor
jason.taylor@manchester.ac.uk

¹ Division of Psychology, Communication and Human Neuroscience, School of Health Sciences, Faculty of Biology, Medicine, and Health, University of Manchester, Manchester Academic Health Science Centre, Manchester, UK

² Division of Psychology and Mental Health, School of Health Sciences, Faculty of Biology, Medicine, and Health, University of Manchester, Manchester Academic Health Science Centre, Manchester, UK

³ Child & Adolescent Mental Health Services, Royal Manchester Children's Hospital, Central Manchester University Hospitals NHS Foundation Trust, Manchester Academic Health Science Centre, Manchester, UK



© The Author(s) 2023. **Open Access** This article is licensed under a Creative Commons Attribution 4.0 International License, which permits use, sharing, adaptation, distribution and reproduction in any medium or format, as long as you give appropriate credit to the original author(s) and the source, provide a link to the Creative Commons licence, and indicate if changes were made. The images or other third party material in this article are included in the article's Creative Commons licence, unless indicated otherwise in a credit line to the material. If material is not included in the article's Creative Commons licence and your intended use is not permitted by statutory regulation or exceeds the permitted use, you will need to obtain permission directly from the copyright holder. To view a copy of this licence, visit <http://creativecommons.org/licenses/by/4.0/>. The Creative Commons Public Domain Dedication waiver (<http://creativecommons.org/publicdomain/zero/1.0/>) applies to the data made available in this article, unless otherwise stated in a credit line to the data.

Background

Neurofibromatosis type 1 (NF1) is an autosomal-dominant neurodevelopmental disorder, present in around 1 in 2700 births [1]. Although there is great inter-individual variability in its clinical manifestations, core somatic symptoms include dermal neurofibromas and pigmentary lesions [2]. In addition to somatic symptoms, social and behavioural difficulties are common, with around 50% of children with NF1 meeting the diagnostic criteria for attention-deficit hyperactivity disorder (ADHD) and around 25% for autism spectrum disorder (ASD) [3]. Moreover, cognitive impairments, including working memory deficits, are prevalent [4] and substantially impair academic achievement [5] and impact negatively on quality of life [6].

There remains a need to better understand the relationship between cortical function and cognitive deficits in NF1 [7] to help provide target(s) for pharmacological and non-pharmacological interventions (e.g. non-invasive brain stimulation [8]; neurofeedback: [9]), which in turn may improve treatment outcomes and academic trajectories. This model is succinctly illustrated by Reinhart and Nguyen [10], albeit in a different context from the present work. Specifically, in their study, neuroimaging revealed uncoupled theta-gamma rhythms during working memory performance in healthy older adults relative to healthy younger adults. In turn the authors used transcranial alternating current stimulation, a non-pharmacological technique, in an attempt to rectify the aberrant cortical functioning in the older adult sample. They reported increased neural synchronisation following intervention and accordingly, improved working memory performance.

Existing neuroimaging research has related cognitive deficits in NF1 to brain function using functional magnetic resonance imaging (fMRI). Studies suggest aberrant activity compared to typically developing controls [7]. For example, increased functional connectivity between the ventral anterior cingulate cortex and the insular cortex during rest may contribute to impaired cognitive control [11]. Aberrant activity has also been observed during cognitive task performance, including reduced task-related activity in key frontal and parietal regions during working memory tasks [12, 13]. Only a limited number of studies have used M/EEG to investigate the neural correlates of cognitive impairments in NF1. Abnormalities in Event Related Potential (ERP) components relative to typically developing controls have been reported [14–18]. For instance, reduced P1 amplitude has been observed, suggesting aberrant early visual processing [14, 18]. Additionally, reduced P3a amplitude has been observed during a go/no-go task and is hypothesised to reflect impaired inhibition [18]. Furthermore,

topographic differences in P3b amplitude and a shorter P3b latency relative to controls have been found during working memory task performance, which the authors suggest may contribute to the cognitive deficits seen in NF1 [16].

The high temporal resolution of M/EEG also enables the study of brain oscillations. Oscillations can be seen as a ‘primary’ or a more direct measure of brain activity relative to ERPs, therefore providing an important window into understanding cognitive processes [19]. As such, investigating oscillations in NF1 can provide additional insights to those gained from ERP methods. Oscillatory measures are particularly well-suited to the investigation of protracted processes [20], such as those required for working memory—a cognitive ability that is impaired in NF1 [16]. Investigations in healthy adults suggest a domain general frontoparietal network supporting working memory performance, irrespective of the modality performed (e.g. visual, auditory, etc.) [21]. In healthy adults, increased (mid-frontal) theta power is observed during working memory maintenance and is hypothesised to maintain the temporal relationship between items held in working memory [22, 23]. Moreover, increased theta phase coherence (i.e. the consistency of phase values between brain regions [24]) between frontal and parietal-temporal regions is observed during working memory maintenance and is thought to facilitate the integration of information between these key regions of the working memory network [25, 26]. The current paper focuses on an adolescent sample, which includes individuals aged 11–16 years. The literature exploring working memory related (WM-related) theta oscillations in typically developing children/adolescents is sparse [27], though there is some evidence to suggest that increased theta band activity occurs during working memory maintenance, like in adulthood [28, 29]. Moreover, the literature suggests that increasing age is associated with a reduction in slow wave resting state power throughout healthy development [30–32] and that power reduction, especially in the theta frequency range, is associated with the development of working memory [31]. For instance, in their study of 6–26-year-olds, Rodriguez-Martinez and colleagues [31] reported a negative correlation between theta power recorded during resting state and working memory performance, suggesting that reductions in resting state slow wave power are linked to enhanced working memory performance with age.

Studies in neurodevelopmental disorders that experience overlapping cognitive impairments with NF1 (e.g. ADHD/ASD [14]) have reported differences in oscillatory activity during working memory performance relative to typically developing controls in both children/adolescents [33, 34] and adult [35, 36] populations. For

instance, Lenartowicz et al. [33] investigated oscillatory activity in children/adolescents aged 7–14 years with a diagnosis of ADHD. Relative to typically developing controls, the ADHD group demonstrated lower alpha event-related desynchronisation during visual encoding of information to be maintained, along with increased mid-frontal theta and occipital alpha event-related synchronisation during working memory maintenance. The authors hypothesise that increased oscillatory activity during maintenance may be a compensatory mechanism employed to counteract the difficulties experienced during encoding. Given that aberrant activity in specific frequency bands exhibits considerable overlap across neurodevelopmental disorders [37], we might also observe abnormalities in WM-related oscillatory activity in the NF1 population.

At present, there are only two existing studies investigating M/EEG oscillatory correlates of cognitive impairments in NF1 [17, 38]. These studies did not investigate activity during working memory task performance, but instead during rest and during visual processing [17] and covert attention tasks [38]. Ribeiro et al. [17] observed higher resting state theta power in NF1 relative to typically developing controls, typical alpha reactivity (i.e. higher alpha power during eyes closed relative to eyes open resting state [39]), and enhanced alpha power during visual processing that may provide a neural marker of attentional deficits in this population. Moreover, Silva et al. [38] found elevated alpha desynchronisation during a covert attention task that may reflect a compensatory mechanism to keep performance at normal levels. Exploration of oscillatory activity in other cognitive domains impaired in NF1, such as working memory, is lacking. Investigating oscillatory activity during working memory is important as working memory underpins and shares common neural correlates with other cognitive functions important to everyday functioning, such as learning [40] and attention [41].

With this in mind, the current study compared EEG power and theta phase coherence in adolescents with NF1 to an age/sex-matched typically developing control group using EEG measured during rest and during a working memory task. Consistent with previous work [17], we hypothesised higher resting state spectral power in NF1, but normal power reactivity during eyes open versus eyes closed resting state conditions. Our analysis of oscillatory activity during working memory was largely exploratory; however, we predicted aberrant theta power and frontoparietal theta phase coherence given previous WM-related EEG studies in other neurodevelopmental disorders [33, 36]. Finally, the association between EEG measures and age, overall adaptive function, and working memory performance was also explored.

Table 1 Eligibility criteria

Eligibility criteria	
NF1	(i) Aged 11–16 years (ii) Satisfied the National Institute of Health's NF1 diagnostic criteria (iii) No history of epilepsy (iv) No ongoing active treatment for any NF1-related complications (e.g. chemotherapy for optic gliomas) (v) No other clinically significant unrelated illness
CON	(i) Aged 11–16 years (ii) No pre-existing medical conditions or neurodevelopmental disorders

Methods

The current study is an extension of the analysis presented in Pobric et al. [16]. Specifically, we conducted oscillatory analyses on the same participants, using the same EEG resting state and n-back data, and used some (see the 'Procedure' section) of the same behavioural measures described in Pobric et al. [16].

Participants

Thirty-two participants completed this study. Participants were adolescents with NF1 ($n=16$) and age- and sex-matched controls ($n=16$). These data were collected as part of a pilot intervention study involving the use of transcranial direct current stimulation (tDCS) [NCT03310996].¹ Post hoc analysis of Ribeiro et al.'s [17] resting state theta effect in NF1 using G*Power [42] suggests that $n=17$ participants per group would result in 79% power to detect an effect size of $d=0.89$. Participants were required to meet each of the eligibility criteria in Table 1.² We selected a pragmatic sample of children with NF1. Previous literature suggests that social communication difficulties (not meeting the criteria for ASD) may be very common affecting up to 60% of children with NF1 [3]. Given how common comorbid neurodevelopmental conditions such as ASD, ADHD, and developmental coordination disorder are in NF1, we decided to include a sample that would be representative of the children seen in the clinic. Parents/guardians gave oral and written consent, and adolescents assent (where developmentally appropriate), prior to participation.

The NF1 sample was recruited through the Manchester Centre for Genomic Medicine, Neurofibromatosis charities, social media platforms, and newsletters

¹ Given the lack of previous safety data with regards to tDCS in this population, we chose a secondary school sample so that the children were able to report any potential side effects.

² Participants' medical records were screened before being invited to take part in the study. None of the participants had a history of traumatic brain injury.

Table 2 Participant demographics

Demographic	Group	
	NF1	CON
Age (M ± SD (range))	13.03 ± 1.66 (11.33–16.92) years	13.34 ± 1.61 (11.25–16.58) years
Sex (male/female)	9/7	9/7
NF1 mutation (inherited/de novo)	7/9	N/A
Medication	Melatonin (n=2) Methylphenidate (n=4)	N/A
Pre-existing clinical diagnoses	ADHD and ASD (n=3) ADHD (n=1) ASD (n=2)	N/A

and were adolescents who satisfied the National Institute of Health's (1988) diagnostic criteria for NF1 [43]. The control sample (CON) was age- and sex-matched at group level and recruited via institutional news-letter advertisements and contacting local schools. Demographic information of the sample is reported in Table 2. There were no significant differences between groups in age ($t_{(30)} = 0.540$, $p = 0.593$) or sex ($\chi^2 = 0.00$, $p = 1.00$).³ In a previous paper reporting on this sample [16], the NF1 group demonstrated poorer performance relative to typically developing controls on various cognitive measures, including measures of working memory (i.e. digit-span forward/backwards) and attention (Sky search attention, TEACH).

Procedure

This study received ethical approval from the Greater Manchester West Research Ethics Committee (17/NW/0364) and was conducted in accordance with the Declaration of Helsinki. During the study visit, participants and their parents/guardians were first familiarised with the EEG equipment and study procedures. Subsequently, a battery of behavioural and cognitive assessments was administered, including parent-rated and cognitive measures that tapped into: overall adaptive function, inattention, hyperactivity, communication, daily living skills, socialisation, short-term memory, working memory, sustained attention, and attentional switching, followed by EEG. This paper focuses on parent-reported⁴ Adaptive Behaviour Composite (ABC) scores on the Vineland Adaptive Behaviour Scale (VABS-III) [44], performance on an adaptive auditory n-back task [16], and performance on a non-adaptive visual n-back task

[16] performed during EEG (see Pobric et al. [16] for details of the other tasks performed that are not reported here).

VABS-II measures daily living skills, socialisation, and communication, with ABC scores reflecting standardised age equivalent overall adaptive functioning [44]. Performance on the adaptive auditory and non-adaptive visual n-back tasks measure working memory. Each trial of the n-back task began with a fixation cross (+) presented in the centre of the screen (adaptive auditory n-back: 2500 ms; non-adaptive visual n-back: 2000 ms, +/- random jitter up to 100 ms in 17 ms steps). This was followed by a single uppercase English consonant (C, G, H, K, P, Q, T, or W) presented aurally (auditory n-back: 1000 ms) or visually in the centre of the screen (non-adaptive visual n-back: 500 ms). Participants were instructed to respond as quickly and accurately as possible with a mouse-click whenever the current stimulus was the same as the one presented 'n' steps back in the sequence. No responses were required for non-targets. The auditory n-back was adaptive, such that after each block of 20 trials, the difficulty level of the next block was adjusted based on the participant's performance to ensure participants were always training at the top of their ability (see Pobric et al. [16] for further task details). In contrast, the visual n-back performed during EEG recording was not designed to push participants' ability to their limit. Instead, it was developed to provide a sufficient number of trials to permit the investigation of electrophysiological differences between the groups during working memory performance. In this non-adaptive task, four fixed-order blocks were presented: 1-back, 2-back, 2-back, and 1-back, with self-paced breaks in between to reduce fatigue. In each block, there were 100 trials, 25 of which were target trials (i.e. the same letter as 'n' screens back). As existing studies report a load-related increase in power during working memory maintenance [45], two load levels ('n' = 1 and 2) were included to permit investigation of load-dependent effects on EEG measures.

³ This remained the case for the sub-group of participants included in the resting state (CON/NF1: $n = 16/14$) and task-specific (CON/NF1: $n = 16/13$) analyses (Additional file 1).

⁴ Parents completed the pen-and-paper version of the Vineland ABC. Adolescent report was not obtained to limit testing burden on the participants.

Table 3 Number of ICA components removed, channels interpolated, and trials remaining

	No. of components removed		No. of channels interpolated		No. of trials remaining ^a			
	M ± SD	Min–Max	M ± SD	Min–Max	Open/1-back		Closed/2-back	
					M ± SD	Min–Max	M ± SD	Min–Max
Resting-state								
CON	1.94 ± 0.44	1–3	1.00 ± 0.00	1–1	75.13 ± 11.63	48–105	71.19 ± 6.39	52–77
NF1	1.86 ± 0.36	1–2	1.00 ± 0.00	1–1	61.43 ± 18.34	22–76	63.64 ± 15.17	32–77
Task-related								
CON	1.69 ± 0.70	1–3	1.50 ± 1.21	1–5	130.55 ± 50.00	46–194	111.88 ± 47.22	38–194
NF1	1.73 ± 0.59	1–3	1.73 ± 1.62	1–6	132.33 ± 46.24	28–188	113.13 ± 53.10	38–195

Abbreviations: M mean, SD standard deviation, Min minimum, Max maximum

^a For task-related data, the number of trials remaining reflects the number of trials after incorrect responses were removed

EEG acquisition

EEG data were recorded using an ActiveTwo system (BioSemi, Amsterdam, Netherlands) with 64 EEG channels in standard 10–10 system locations plus HEOG, VEOG, and mastoids, with a sampling rate of 512 Hz. During the recording, participants were asked to remain still, in a comfortable/relaxed position, and to minimise eye movements and blinking where possible. Recording started with 2.5 min of eyes open and 2.5 min of eyes closed resting state, in which participants were asked to simply relax and not think of anything in particular. This was followed by recording during the visual n-back task.

EEG analysis

MATLAB (2019a) and SPM12 (version 7771) were used to conduct data analyses. Custom functions [46, 47] calling several functions from EEGLAB (version 13.6.5b) and FieldTrip (embedded in SPM release) were used.

Common pre-processing

Continuous EEG data were re-referenced to averaged mastoids, high-pass filtered (0.1 Hz), downsampled (256 Hz), low-pass filtered (resting state: 200 Hz; task-related: 120 Hz), and notch-filtered (48–52 Hz), before epoching (resting state: arbitrary 1900 ms (baseline correction: 0–1900 ms, i.e. mean-centring); task-related: 0–1900 ms relative to stimulus onset). The eyes open and eyes closed data were then concatenated (i.e. combined into the same file).

Independent component analysis (ICA) was used to project blink and eye-movement signals out of the data.⁵

Channels containing noise unrelated to blinks (characterised by large positive deflections) or eye movements (characterised by square-wave deflections) were temporarily omitted (channel TP7 was persistently bad and omitted from ICA for all participants). Thirty-two components were extracted from EEG channel data only. ICA components with uniquely high temporal correlations with VEOG and HEOG, and/or uniquely high spatial correlations with the blink topography, were identified using custom code [46] and following the procedure described in Pobric et al. [16]. The resulting weight matrix (less the artefact components) was applied to the epoched data using SPM12's 'montage' function.

Baseline correction was then re-applied on the ICA-cleaned data. Epochs were rejected as noisy if they contained signal that exceeded a threshold (resting state: 200 µV; task-related: 120 µV; higher threshold for resting state data due to higher alpha power during eyes closed resting state). A channel was declared 'bad' if the threshold was exceeded on >20% of trials, and epoch rejection was re-run ignoring any bad channels. To reconstruct these noisy channels, a channel-weight interpolation matrix was created using FieldTrip's 'channelrepair' function and applied to the epoched data using SPM12's 'montage' function. EEG data were then re-referenced to the common average reference. The mean number of components removed, channels interpolated, and trials remaining can be seen in Table 3.

Resting state analysis

To be eligible for inclusion, participants were required to have a minimum of 15 valid epochs remaining in each condition (open/closed) after artefact-contaminated trials were removed. Two participants were excluded from the NF1 group, one due to having fewer than 15 valid trials in the eyes open condition and the other due to low-quality data (i.e. all channels automatically marked 'bad'

⁵ Note, the use of ICA for artefact signal removal does not pose a problem for phase-based analyses such as coherence [78]. ICA is an instantaneous spatial filtering method, and as such it does not distort the phases of the underlying signals. There may, however, be *apparent* changes in phase of *channel* data after removing artefact components since channels contain weighted sums of underlying neural and artefact signals (some of which have been removed). In fact, after artefact removal, channel data should be a purer measure of neural source data, including the oscillations of interest here.

during the artefact detection routine). The sample used for the resting state analyses therefore comprised 30 participants ($n = 16$ CON; $n = 14$ NF1).

Task-related analysis

Trials with incorrect responses were excluded. Subsequent analyses were conducted on target and non-target trial data without distinguishing between these conditions, since n-back performance requires maintenance of information during both trial types, particularly in the late post-ERP time window (described below). For the same reason, the number of non-target trials was not decimated to match the number of target trials (which was done in the P300 analysis presented by Pobric et al. [16]).

To be eligible for inclusion participants were required to have a minimum of 15 valid epochs remaining in each load (1-/2-back) after artefact-contaminated trials and incorrect trials were removed. One participant from the NF1 group was excluded owing to having fewer than 15 valid trials in the 2-back load level (this was a different participant from the two resting state exclusions). The sample size used for the task-related analyses therefore comprised 31 participants ($n = 16$ CON; $n = 15$ NF1).

Spectral power

For estimation of task-related power, the time window of interest was 900–1900 ms post-stimulus onset (i.e. during the fixation cross of the next trial). This time window was chosen as existing studies investigating WM-related oscillatory activity typically use the maintenance period of the working memory task as the time window of interest as increased oscillatory activity is observed during this period [22, 26, 36, 48]. We followed the previous literature's definition of the maintenance period as the time following a response to the stimuli, determined using the average (or median) response time on the given task [36]. In the current study, the average response time over 1-/2-back blocks was 627 ± 124 ms (median: 601 ms). However, to ensure that the majority of participants had responded, 900 ms was chosen as the beginning of the time window. The time window ended at 1900 ms to provide a sufficient number of samples for power estimation. For consistency, the same time window (in the arbitrary epoch), and therefore number of samples, was used for the estimation of resting state power.

For each EEG channel and epoch (resting state: eyes open and eyes closed; task-related: 1-back and 2-back), a Fast Fourier Transform with a Hanning window and a frequency resolution of 1 Hz was used to extract frequency spectra collapsed over time (900–1900 ms). The

resulting power values were then log-transformed before averaging spectra over epochs. For exploratory analysis, average log-transformed power over all EEG channels was computed in canonical frequency bands: delta: 1–3 Hz; theta: 4–7 Hz; alpha: 8–11 Hz; beta: 12–29 Hz; low-gamma: 30–47 Hz, and high-gamma: 53–100 Hz. Additionally, as the literature consistently reports increased mid-frontal theta power during working memory maintenance [22], we performed targeted analysis of task-related mid-frontal theta (4–7 Hz) power. To achieve this, log-transformed power was averaged over channels Fz, F1, and F2 to create a mid-frontal region of interest prior to statistical analysis. We measured absolute power (i.e. power in one frequency band, independent of activity in other frequency bands), as opposed to relative power (i.e. power in one frequency band divided by the amount of activity in all frequency bands) to avoid the potential confound that any abnormalities in one frequency band may affect the relative power of other frequency bands—a particular concern in neurodevelopmental disorder studies [49].

Peak alpha frequency

Differences in peak alpha frequency (PAF) between groups were investigated. PAF was defined as the frequency with the maximum power in a loose alpha range (6.5–13.5 Hz) at channel Pz. Pz was chosen as alpha power is typically high at this channel [50]. For analysis of PAF, for each EEG channel and epoch (eyes open/closed), a Fast Fourier Transform with a Hanning window and a frequency resolution of 0.25 Hz was used to extract frequency spectra collapsed over time (arbitrary 1900 ms epoch). First, each individual's 1D spectrum was adjusted to reduce 1/f noise as this flattens the spectrum and causes the alpha peak to 'pop out' [51]. This was achieved by fitting a second-order polynomial to the log-transformed frequencies (omitting alpha and notch-filter frequencies), and the difference between the spectrum and this model was computed. The resulting spectrum was smoothed with a Gaussian kernel to remove spurious peaks. Next, four adjustments were made based on visual inspection of each participant's spectrum: Two CON and one NF1 participant had maxima that fell on the ascending slope of the beta peak (eyes open: 12.25 Hz, 13.25 Hz, and 12.75 Hz; eyes closed: 13.25 Hz, 12.75 Hz), and these were adjusted to small visible alpha peaks (eyes open: 11.50 Hz, 10.25 Hz, and 10.75 Hz; eyes closed: 11.75 Hz, 11.75 Hz) that our algorithm had missed, and one NF1 participant's maximum fell on the descending delta slope (eyes open and closed: 6.5 Hz) and was adjusted to small visible alpha peaks (eyes open: 7 Hz, eyes closed: 7.5 Hz) missed by the algorithm.

Theta phase coherence

Prior to estimating phase coherence, the task-related data were spatially filtered using the Surface Laplacian, implemented using the `laplacian_perrinX` function in MATLAB [52]. The Surface Laplacian reduces the influence of volume conduction, which is particularly important given the electrode-level connectivity analysis performed [53]. We investigated theta phase coherence in the frontoparietal network (Fig. 1). The mid-frontal region acted as a seed region and coherence was estimated between this region and left-parietal, mid-parietal, and right-parietal regions [54]. Each region comprised of a set of electrodes: mid-frontal (F1/Fz/F2), left-parietal (P3/P5/P7), mid-parietal (P1/Pz/P2), and right-parietal (P4/P6/P8). Coherence was estimated between each possible mid-frontal–parietal connection (i.e. 27 channel pairs), before averaging coherence over electrode sets, resulting in three coherence estimates: mid-frontal to (1) left-parietal (ML), (2) mid-parietal (MM), and (3) right-parietal (MR).

Theta phase was computed for the whole epoch (0–1900 ms) and then phase coherence was computed in the time window of interest, 900–1500 ms post-stimulus (the time window ended at 1500 ms to prevent inclusion of edge effects as per epoch definition). We calculated inter-site phase clustering (ISPC) [20]. ISPC over trials is a measure of the consistency of phase angles between two electrodes averaged over trials. For task-related data, ISPC-trials is an appropriate method given our analysis is hypothesis-driven (i.e. limited to the frontoparietal network) and not exploratory (more suited to weighted phase lag index) [20]. ISPC has

been used previously in studies with similar methodology [54]. Phase angle time series for each channel was extracted by convolving the data with a complex Morlet wavelet (4 cycles) separately for frequencies 4 Hz, 5 Hz, 6 Hz, and 7 Hz. For each time point, the average vector length was calculated across trials to quantify ISPC trials, defined as:

$$ISPC_f = \left| n^{-1} \sum_{t=1}^n e^{i(\phi_{xt} - \phi_{yt})} \right| \quad (1)$$

where n represents the number of trials and ϕ_x and ϕ_y are phase angles from channels x and y at frequency f . ISPC ranges from 0 (perfectly randomly distributed phases) to 1 (perfect phase-locking). For each channel pair, ISPC trials were calculated for each load (1-/2-back) and frequency (4–7 Hz). The result was then averaged over the time window of interest (900–1500 ms post-stimulus), then over frequencies, and finally over channel sets. This resulted in one coherence value for each frontoparietal region pair/load combination (ML, MM, MR × 1-back, 2-back) for each participant.

Statistical analysis

Statistical analyses were conducted using SPSS (Version 25). The alpha level was set to 0.05. Visual inspection of Q-Q plots showed that, for each analysis, data were normally distributed. For each analysis of variance discussed below, Box and Whisker plots were inspected for extreme outliers. Values were considered extreme outliers if they fell outside of 3rd quartile + 3*interquartile range and 1st

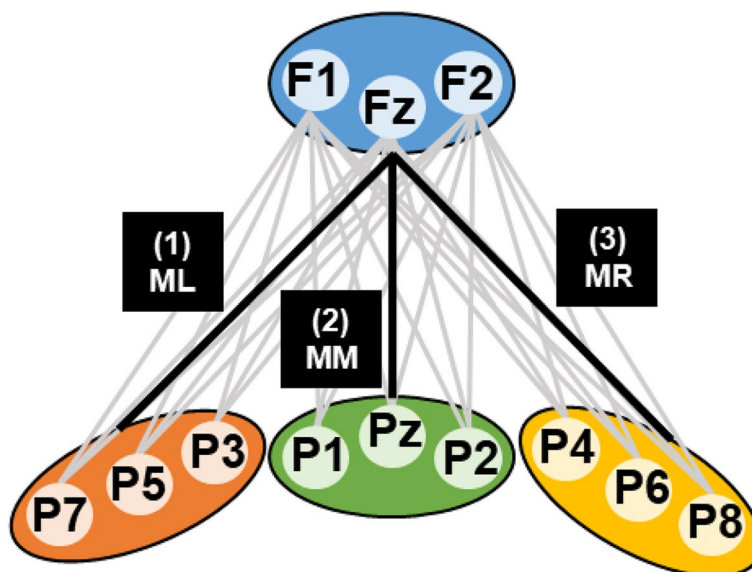


Fig. 1 Graphical representation of the channels included in each region of interest. Grey lines indicate the 27 channel pairs that coherence was computed between. Black lines represent coherence averaged over electrode sets (ML: mid-frontal to left-parietal; MM: mid-frontal to mid-parietal; MR: mid-frontal to right-parietal)

quartile – 3*interquartile range. Where extreme outliers were identified, sensitivity analyses were run. It can be assumed that there were no extreme outliers identified where sensitivity analysis is not reported.

In each frequency band, a 2 (CON/NF1) × 2 (open/closed) analysis of variance (ANOVA) was run for the scalp-averaged resting state data. ANOVAs were run separately for each frequency band as there is a known 1/f effect, whereby the means of low frequencies are larger than those of high frequencies [55]. As frequency bands are estimated independently, and therefore each ANOVA is performed on independent data, no correction for multiple comparisons was used. Moreover, to investigate whether resting state power follows the typical reactivity pattern observed in neurotypical populations [39], in each frequency band a paired *t*-test investigated power differences between eyes open and eyes closed resting state in the NF1 group. A 2 (CON/NF1) × 2 (open/closed) ANOVA was also used to analyse PAF.

In the n-back task, maintenance of items in working memory spans trials. We therefore used eyes-open resting state recordings as a baseline to investigate task-specific power modulation (i.e. change from rest). To achieve this, we divided task-related power by resting state power before log-transforming the data⁶ (equivalent to: $\log(\text{task power}) - \log(\text{resting state power})$), which is referred to as *task-specific* power henceforth. In each frequency band, a 2 (CON/NF1) × 2 (1-/2-back) ANOVA investigated scalp-averaged task-specific power. Consistent with the task-related power analyses, we investigated task-specific theta phase coherence by adjusting for baseline (resting state). For comparability, eyes open resting state theta phase coherence was estimated using the same method as task-related phase coherence (note the ‘trials’ in ISPC-trials are arbitrary in resting state). Prior to statistical analysis, resting state phase coherence was subtracted from task-related phase coherence. A 2 (CON/NF1) × 3 (ML/MM/MR) × 2 (1-/2-back) ANOVA using task-specific frontoparietal theta phase coherence was performed.

As existing research suggests a significant relationship between age and oscillatory activity in typically developing children that may not be present in neurodevelopmental disorders [56], Pearson’s correlations were performed to investigate associations between EEG measures and age, followed by statistical significance testing of the difference in *r* between groups to determine whether the relationship between age and

oscillatory activity was significantly different between groups. This was achieved using Fisher’s *r* to *z* transformation, before statistically comparing the resulting *z* scores. Moreover, as individuals with NF1 typically exhibit worse overall functioning relative to typically developing children [6, 57], and there is suggestion that oscillatory activity might be a neural marker of cognitive function in neurodevelopmental disorders [56], Pearson’s correlations were performed to investigate associations between EEG measures and overall adaptive functioning, using Vineland ABC scores. Again, this was followed by statistical significance testing of the difference in *r* between groups to determine whether the relationship between overall adaptive function and oscillatory activity was significantly different between groups. Finally, to assist interpretation of the oscillatory findings, Pearson’s correlations were performed to investigate associations between EEG measures and working memory performance on the adaptive auditory n-back task (which was conducted separately to the EEG session), and the difference in *r* between groups compared. To correct for multiple comparisons, a 5% false discovery rate (FDR) [58] correction was applied to outcomes with *p*-values less than 0.05. FDR was applied to the set of EEG measures for each demographic/behavioural domain (i.e. five *p*-values).

Results

Behavioural

As expected, NF1⁷ performed significantly worse than CON on the parent-rated Vineland ABC ($t_{(29)} = 3.573$, $p < 0.001$) and adaptive auditory n-back task (mean n-back; $t_{(30)} = 5.412$, $p < 0.001$). Moreover, the NF1 group did not demonstrate any impairment in EEG n-back task performance (hits – false alarms (%); $F_{(1,30)} = 0.094$, $p = 0.762$, $\eta_p^2 = 0.003$) (see Additional file 1 for detailed reporting).

Resting state power: higher delta and theta power in NF1

Figure 2 displays spectral power as a continuous spectrum (top), and averaged in canonical frequency bands (middle), both averaged over all EEG channels, and as topographic maps (bottom) during (a) eyes open and (b) eyes closed resting state.

Visual inspection shows that spatial distributions were similar between CON and NF1 in all frequency bands, but with greater magnitudes in NF1 relative to CON.

⁶ To calculate task-specific power and phase coherence participants needed to be eligible for both resting state and task-related analyses. This reduced the sample size from $N = 31$ (CON/NF1: $n = 16/15$) to $N = 29$ (CON/NF1: $n = 16/13$).

⁷ These findings remained the same when the analyses were run on the sample eligible for inclusion (see the ‘EEG analysis’ section) in the resting state ($N = 30$), task-related ($N = 31$), and task-specific analyses ($N = 29$) reported in the current paper (Additional file 1).

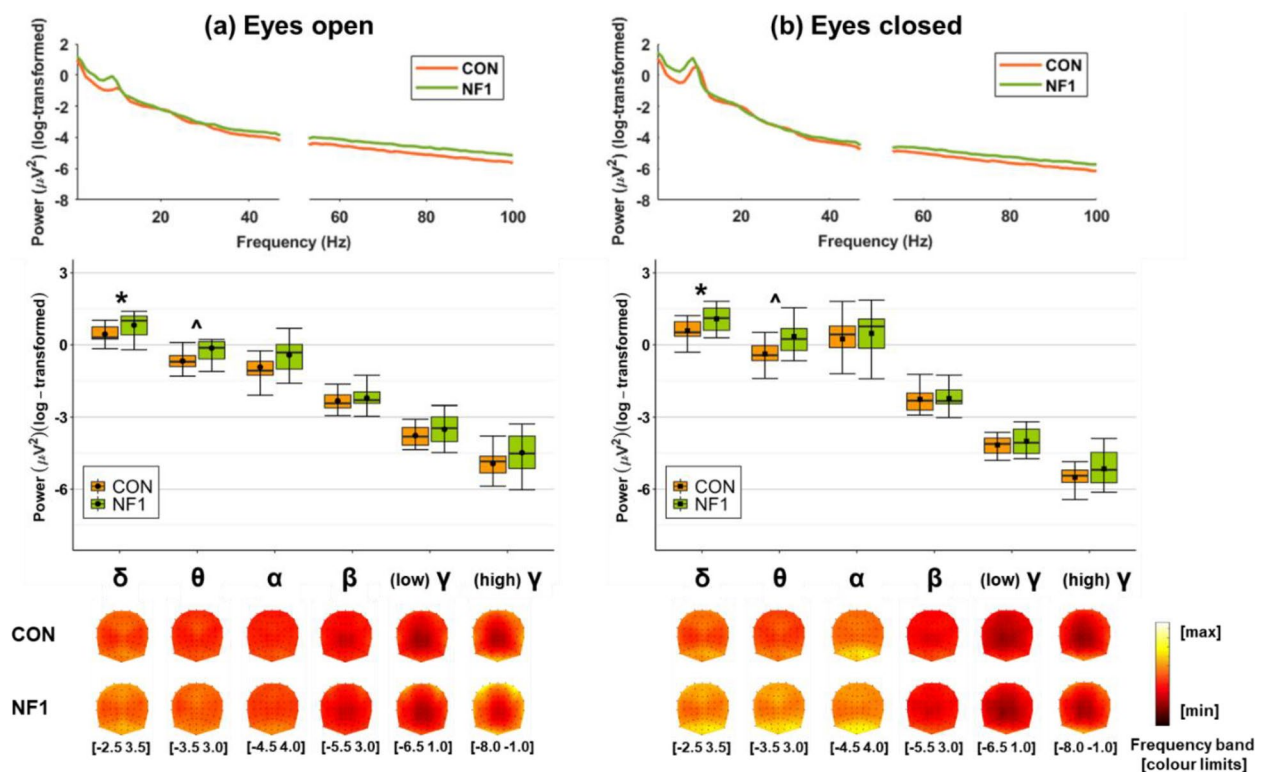


Fig. 2 Grand-averaged log-transformed spectral power during rest with **a** eyes open and **b** eyes closed. Spectral power is shown as a continuous spectrum (top) and averaged in canonical frequency bands (middle), both averaged over all EEG channels, and as topographic maps (bottom). (Abbreviations: δ : delta, 1–3 Hz; θ : theta, 4–7 Hz; α : alpha, 8–11 Hz; β : beta, 12–29 Hz; (low) γ : low-gamma, 30–47 Hz; (high) γ : high-gamma, 53–100 Hz. Box plots: crossbars represent the median, dots represent the mean, upper and lower hinges correspond to the 1st and 3rd quartile, respectively, and whiskers represent the range of the data. * and ^ significant main effect of group in the delta and theta bands, respectively, collapsed over condition)

Moreover, greater magnitudes are seen during eyes closed relative to eyes open for delta, theta, and alpha, whilst the opposite pattern is observed for low-gamma and high-gamma. The difference in power between groups was significant for delta ($F_{(1,28)}=7.135$, $p=0.012$, $\eta_p^2=0.203$) and theta ($F_{(1,28)}=9.145$, $p=0.005$, $\eta_p^2=0.246$), but non-significant for alpha, beta, low-gamma, and high-gamma (Table 4, Fig. 2).

There were significant main effects of condition for delta, theta, alpha, low-gamma, and high-gamma, where power was significantly higher during eyes closed relative to eyes open for delta, theta, and alpha, but power was significantly higher during eyes open relative to eyes closed for low-gamma and high-gamma. The absence of significant group \times condition interactions in these frequency bands suggests that modulation of amplitude of the oscillations did not differ between groups. Planned paired t -tests to examine oscillatory reactivity in the NF1 group showed that power was significantly higher during

eyes closed relative to eyes open for delta ($t_{(13)}=5.004$, $p<0.001$, $d=1.34$), theta ($t_{(13)}=4.296$, $p=0.001$, $d=1.15$), and alpha ($t_{(13)}=5.291$, $p<0.001$, $d=1.41$), whilst power was significantly higher during eyes open relative to eyes closed for low-gamma ($t_{(13)}=4.457$, $p=0.001$, $d=1.17$) and high-gamma ($t_{(13)}=4.204$, $p=0.001$, $d=1.12$). There was no significant difference in power between eyes open and eyes closed for beta ($t_{(13)}=0.285$, $p=0.780$, $d=0.08$).

Peak alpha frequency: lower PAF in NF1

Figure 3 illustrates the alpha range of grand average (a) eyes open and (b) eyes closed resting state after adjustment to reduce 1/f noise and the application of Gaussian smoothing. There was a significant difference in PAF between groups ($F_{(1,28)}=12.276$, $p=0.002$, $\eta_p^2=0.305$), whereby compared to CON, NF1 showed a lower PAF (Table 4). There was no main effect of condition, and no group \times condition interaction.

Table 4 Power and PAF: descriptive and inferential statistics

	Eyes open/1-back		Eyes closed/2-back		ANOVA									
	CON	NF1	CON	NF1	Group			Condition/load			Group x Condition/load			
	M±SD	M±SD	M±SD	M±SD	F	p	η ²	F	p	η ²	F	p	η ²	
Resting state					(1,28)			(1,28)			(1,28)			
Delta	0.44±0.38	0.82±0.48	0.58±0.43	1.08±0.52	7.135	.012*	.203	38.371	<.001***	.578	3.299	.080	.105	
Theta	-0.67±0.39	-0.14±0.65	-0.38±0.47	0.35±0.82	9.145	.005**	.246	46.213	<.001***	.623	2.853	.102	.092	
Alpha	-0.93±0.73	-0.43±0.78	0.24±0.92	0.47±0.95	1.609	.215	.054	96.219	<.001***	.775	1.663	.208	.056	
Beta	-2.34±0.45	-2.22±0.48	-2.27±0.52	-2.24±0.55	0.188	.668	.007	0.266	.610	.009	0.954	.337	.033	
Low gamma	-3.77±0.44	-3.51±0.61	-4.16±0.37	-4.01±0.60	1.457	.238	.049	44.477	<.001***	.614	0.630	.434	.022	
High gamma	-4.93±0.55	-4.48±0.84	-5.50±0.45	-5.15±0.76	3.340	.078	.107	43.575	<.001***	.609	0.286	.597	.010	
PAF (Pz)	10.06±1.15	8.64±1.10	9.95±0.87	8.95±1.14	12.276	.002**	.305	0.290	.594	.010	1.313	.261	.045	
Task-specific (adjusted)					(1,27)			(1,27)			(1,27)			
Delta	0.07±0.19	-0.05±0.28	0.15±0.29	-0.01±0.22	2.667	.114	.090	1.767	.195	.061	0.215	.646	.008	
Theta	0.04±0.20	-0.05±0.33	0.09±0.20	-0.04±0.35	1.374	.251	.048	0.660	.424	.024	0.168	.685	.006	
Alpha	0.00±0.33	-0.06±0.46	0.06±0.34	-0.06±0.52	0.398	.533	.015	0.770	.388	.028	0.508	.482	.018	
Beta	0.01±0.24	-0.04±0.19	0.09±0.26	-0.04±0.21	1.252	.273	.044	3.410	.076	.112	2.969	.096	.099	
Low gamma	-0.67±0.32	-0.12±0.38	0.01±0.38	-0.09±0.31	0.396	.535	.014	1.976	.172	.068	0.484	.492	.018	
High gamma	-0.44±0.41	-0.14±0.50	0.08±0.47	-0.14±0.45	0.951	.338	.034	0.990	.329	.035	1.301	.264	.046	
Mid-frontal theta (Fz/F1/F2)	0.03±0.33	-0.10±0.39	0.10±0.27	0.04±0.48	0.598	.446	.022	2.505	.125	.085	0.317	.578	.012	

Abbreviations: M mean, SD standard deviation. ***p < .001, **p < .01, *p < .05. Power (log(μV²)) is averaged over all EEG electrodes unless otherwise specified. Note: the degrees of freedom for resting state (1,28) and task-specific (1,27) analyses are different due to the different number of participants included in each analysis

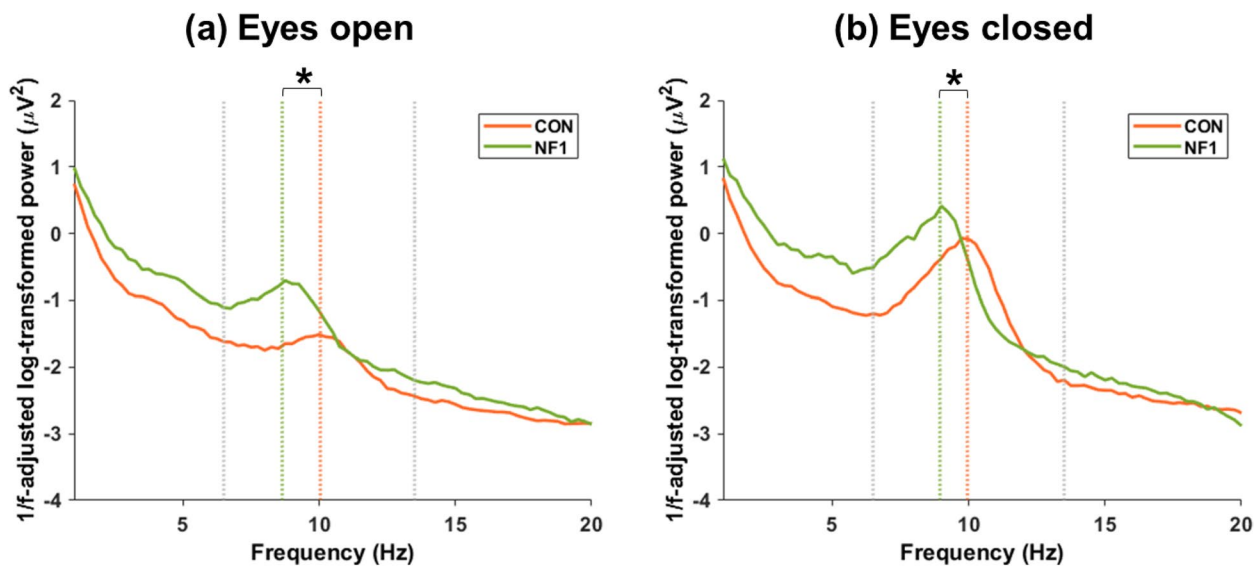


Fig. 3 Grand-averaged 1/f-adjusted log-transformed spectral power during rest. **a** Eyes open and **b** eyes closed. (Grey dashed vertical lines at 6.5 Hz and 13.5 Hz represent the boundaries of the loose alpha range for PAF determination; orange and green dashed vertical lines represent the mean PAF for CON and NF1, respectively; * significant main effect of group collapsed over condition)

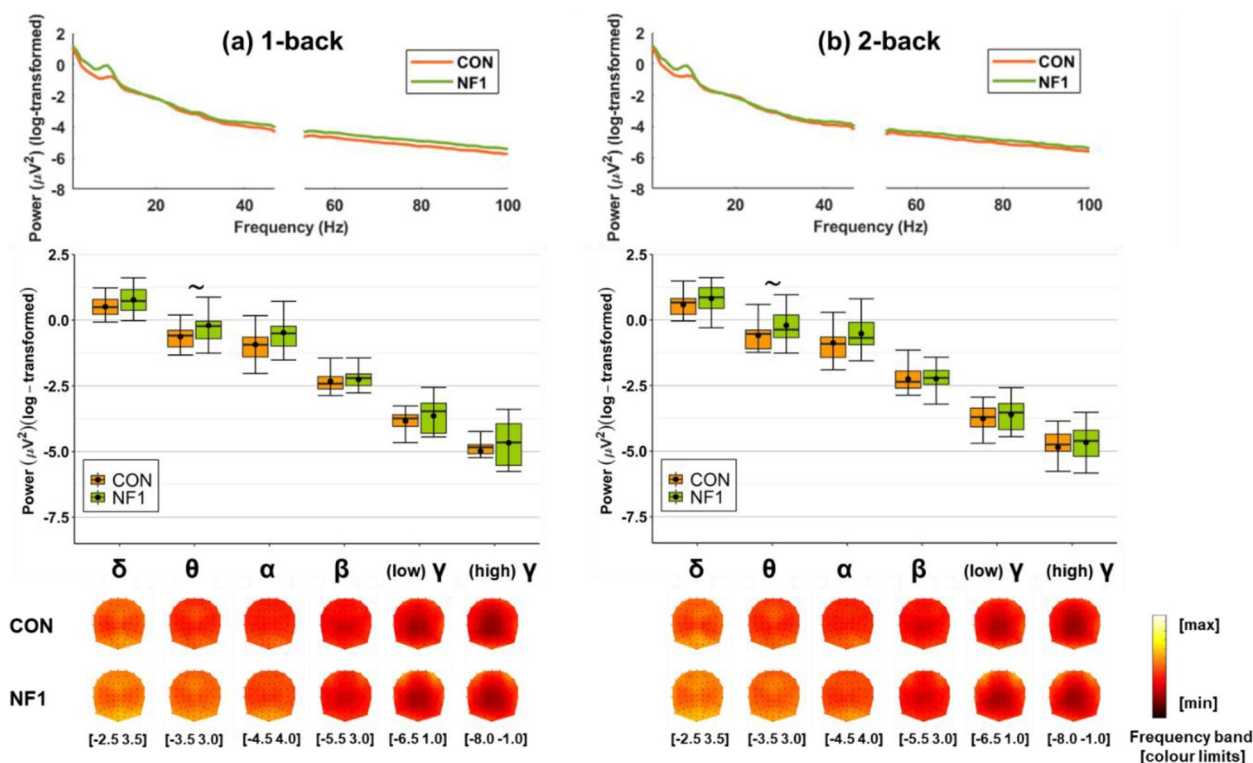


Fig. 4 Grand-averaged log-transformed spectral *unadjusted* power during **a** 1-back and **b** 2-back loads. Spectral power is shown as a continuous spectrum (top) and averaged in canonical frequency bands (middle), both averaged over all EEG channels, and as topographic maps (bottom). (Abbreviations: δ : delta, 1–3 Hz; θ : theta, 4–7 Hz; α : alpha, 8–11 Hz; β : beta, 12–29 Hz; (low) γ : low-gamma, 30–47 Hz; (high) γ : high-gamma, 53–100 Hz. Box plots: crossbars represent the median, dots represent the mean, upper and lower hinges correspond to the 1st and 3rd quartile, respectively, and whiskers represent the range of the data. ~ marginally significant main effect of group in the theta band, collapsed over load level)

Task-related power: no group difference in task-specific power

Figure 4 displays *unadjusted* spectral power as a continuous spectrum (top), and averaged in canonical frequency bands (middle), both averaged over all EEG channels, and as topographic maps (bottom) during (a) 1-back and (b) 2-back load levels.

Visual inspection shows that spatial distributions were similar between CON and NF1 in all frequency bands, but with greater magnitudes in NF1 relative to CON. This group difference in *unadjusted* spectral power was marginally significant for theta only ($F_{(1,29)} = 4.092, p = 0.052, \eta_p^2 = 0.124$) (*unadjusted* power analyses are reported in Additional file 2). To investigate task-specific modulation, we used task-related power adjusted for resting state eyes open power. Note, conclusions cannot be drawn about the absolute value of this difference (i.e. whether task-related is higher or lower than resting state activity) in the absence of a pre-stimulus baseline period in the n-back task. The 2 (CON/NF1) \times 2

(1-/2-back) ANOVA⁸ showed no significant main effects or interactions in any frequency band (Table 4). Thus, the marginal task-related difference in theta power disappeared when accounting for resting-state theta power.

In line with the scalp-averaged *unadjusted* power, mid-frontal *unadjusted* theta power was numerically higher in NF1 than CON (Fig. 5),⁹ though this group difference was non-significant ($F_{(1,29)} = 2.850, p = 0.102, \eta_p^2 = 0.089$) (Additional file 2). Similarly, the 2 (CON/NF1) \times 2 (1-/2-back) ANOVA using task-specific (*adjusted*) theta power showed no significant main effects or interactions (Table 4).

Theta phase coherence: no group difference in task-specific phase coherence

Visual inspection of Fig. 6 shows that *unadjusted* frontoparietal theta phase coherence was numerically higher in NF1 relative to CON in all regions of the frontoparietal network during (a) 1-back and (b) 2-back loads. This group difference in *unadjusted* theta phase coherence was significantly different ($F_{(1,29)} = 4.852, p = 0.036,$

⁸ One extreme outlier was identified in the NF1 group (beta 2-back) from inspection of Box and Whisker plots. After removing this participant from the beta ANOVA, the findings stayed the same (i.e. no significant main effects or interactions).

⁹ Resting state mid-frontal theta power descriptive and inferential statistics are reported in Additional file 3.

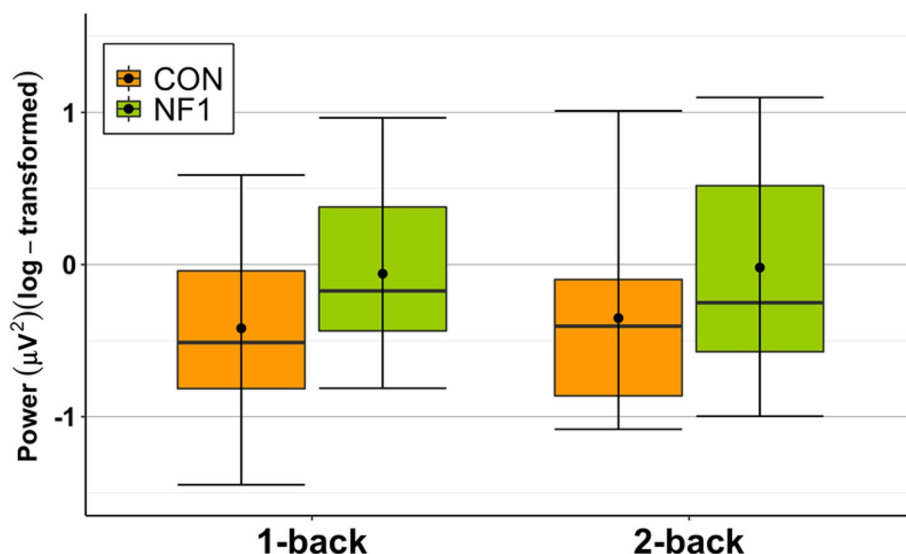


Fig. 5 Grand-averaged log-transformed mid-frontal theta (4–7 Hz) *unadjusted* power during **a** 1-back and **b** 2-back loads. (Box plots: crossbars represent the median, dots represent the mean, upper and lower hinges correspond to the 1st and 3rd quartile, respectively, and whiskers represent the range of the data)

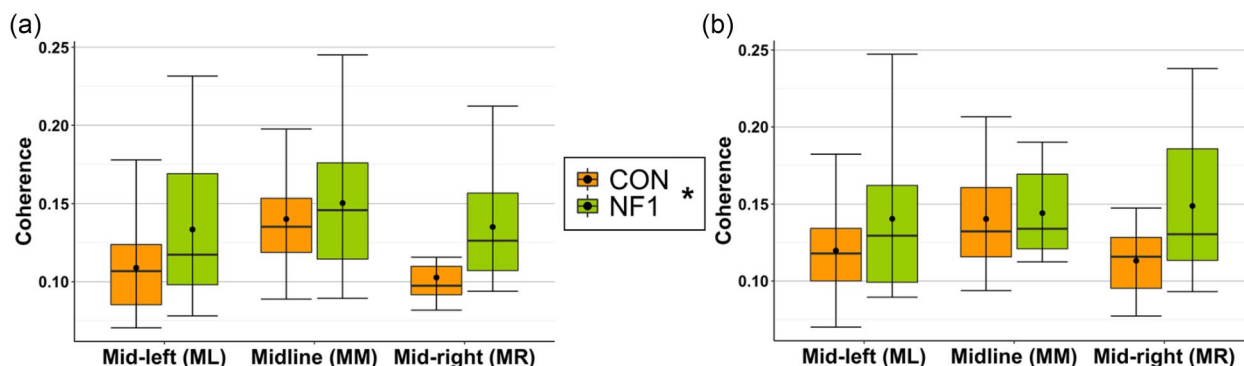


Fig. 6 Box plots display *unadjusted* frontoparietal theta phase coherence during **a** 1-back and **b** 2-back loads. Mid-left (mid-frontal–left-parietal), midline (mid-frontal–mid-parietal), and mid-right (mid-frontal–right-parietal). (Crossbars represent the median, dots represent the mean, upper and lower hinges correspond to the 1st and 3rd quartile, respectively, and whiskers represent the range of the data. *significant main effect of group averaged over region and load)

$\eta_p^2=0.143$) (Additional file 2). However, the 2 (CON/NF1) \times 3 (ML/MM/MR) \times 2 (1-/2-back) ANOVA¹⁰ using task-specific (*adjusted*) theta phase coherence showed no significant main effects or interactions involving the factor ‘group’ (Table 5).¹¹ Again, conclusions cannot be drawn about the absolute value of this difference (i.e. whether task-related is higher or lower than resting state activity) in the absence of a pre-stimulus baseline period in the n-back task. Although not of primary interest, there was a significant region \times load interaction

($F_{(2,54)}=5.023$, $p=0.010$, $\eta_p^2=0.157$). There were no other significant main effects or interactions.

Correlations between EEG measures and age/cognitive measures

Exploratory Pearson’s correlations were run separately for each group to relate individual differences in EEG oscillatory measures with age, overall adaptive function (Vineland ABC), and working memory performance (adaptive auditory n-back)¹² (Table 6, see Additional

¹⁰ Two extreme outliers were identified in the NF1 group (ML 2-back) from inspection of Box and Whisker plots. After removing these outliers, the findings remained the same (i.e. a significant region \times load interaction but no other significant main effects or interactions).

¹¹ Resting state theta phase coherence descriptive and inferential statistics are reported in Additional file 3.

¹² We ran correlations between EEG measures and performance on the digit span forward and digit span backward tasks (we thank a reviewer for this suggestion). There were three significant negative correlations in the CON group, none of which survived FDR correlation (eyes open delta: $r=-.500$, $p=.049$, $q=.082$, eyes closed delta: $r=-.539$, $p=.031$, $q=.082$, and eyes closed theta: $r=-.519$, $p=.039$, $q=.082$).

Table 5 Theta phase coherence (adjusted): descriptive and inferential statistics

Descriptive statistics					
Region	Load	Group	M ± SD		
Mid-frontal–left-parietal (ML)	1-back	CON	−0.014 ± 0.028		
		NF1	−0.020 ± 0.041		
	2-back	CON	−0.003 ± 0.032		
		NF1	−0.014 ± 0.055		
Mid-frontal–mid-parietal (MM)	1-back	CON	−0.003 ± 0.023		
		NF1	0.006 ± 0.049		
	2-back	CON	−0.003 ± 0.034		
		NF1	−0.005 ± 0.035		
Mid-frontal–right-parietal (MR)	1-back	CON	−0.022 ± 0.026		
		NF1	−0.131 ± 0.021		
	2-back	CON	−0.120 ± 0.032		
		NF1	−0.003 ± 0.042		
ANOVA			$F_{(1,27)/(2,54)}$	p	η_p^2
Group			0.028	.868	.001
Region			1.376	.261	.048
Load			1.505	.231	.053
Group × region			0.656	.523	.024
Group × load			0.580	.453	.021
Region × load			5.023	.010*	.157
Group × region × load			0.503	.608	.018

Abbreviations: M mean, SD standard deviation

* $p < .05$. Degrees of freedom: (1,27), (2,54)

file 4 for scatterplots). Correlations were run only for EEG measures that showed a significant group difference in the analyses reported above (i.e. delta and theta resting state power and PAF). For correlations with resting state power, as there was a significant main effect of condition for the delta and theta bands, correlations were run separately for eyes open and eyes closed power. There was

no significant main effect of condition for PAF, so PAF was averaged over eyes open/closed prior to running correlations.

For CON, four negative age-power correlations survived FDR correction: eyes open delta ($r = -0.600$, $p = 0.014$, $q = 0.018$), eyes closed delta ($r = -0.705$, $p = 0.002$, $q = 0.005$), eyes open theta ($r = -0.547$, $p = 0.028$, $q = 0.028$), and eyes closed theta ($r = -0.674$, $p = 0.004$, $q = 0.007$). The same correlations for NF1 were non-significant and group differences in these correlations were non-significant. Moreover, age showed a positive correlation with PAF for CON ($r = 0.736$, $p = 0.001$, survived FDR correction, $q = 0.005$). The same correlation for NF1 was non-significant ($r = -0.241$, $p = 0.407$) and the group difference in these correlations was significant ($z = 4.238$, $p < 0.001$, survived FDR correction, $q = 0.005$). Finally, there were no significant correlations between any of the EEG measures and overall adaptive function (ABC) or working memory performance.

Discussion

This study investigated oscillatory activity during both rest and performance of a working memory task in an adolescent sample with NF1 and age/sex-matched typically developing controls. Relative to controls, NF1 showed higher resting state delta and theta power, and these differences were not modulated by eyes open/closed condition (no group × condition interactions were found). Resting state delta and theta power showed significant negative correlations with age in controls, but not in NF1. NF1 also showed lower PAF than controls, and the positive age-PAF correlation found in controls was not present in NF1 (and these correlations differed significantly between groups). In the working memory task, a marginal group difference in theta power was

Table 6 Correlations between EEG measures and age, Vineland ABC, and working memory

Demographic/ cognitive measure	Group	Resting state				
		Delta power		Theta power		PAF
		Open	Closed	Open	Closed	
Age (years)	CON (r, p)	-.600 (.014)*	-.705 (.002)*	-.547 (.028)*	-.674 (.004)*	.736 (.001)*
	NF1 (r, p)	-.420 (.134)	-.341 (.233)	-.276 (.339)	-.108 (.714)	-.241 (.407)
	CON vs. NF1 (z, p)	-.345 (.730)	-.0745 (.456)	-.0474 (.635)	-.1041 (.298)	4.238 (<.001)*
Vineland ABC	CON (r, p)	-.243 (.364)	-.256 (.339)	-.085 (.756)	-.205 (.445)	.127 (.639)
	NF1 (r, p)	-.066 (.831)	-.040 (.897)	.144 (.638)	.082 (.790)	.149 (.627)
	CON vs. NF1 (z, p)	-.432 (.666)	-.0354 (.724)	-.0431 (.666)	-.0498 (.618)	-0.048 (.961)
Auditory n-back	CON (r, p)	-.265 (.322)	-.220 (.414)	-.197 (.464)	-.159 (.557)	.474 (.063)
	NF1 (r, p)	-.208 (.476)	-.156 (.593)	-.328 (.252)	-.245 (.399)	-.088 (.764)
	CON vs. NF1 (z, p)	-.092 (.926)	-.0103 (.918)	0.213 (.831)	0.140 (.888)	1.505 (.132)

Power is scalp-averaged over all EEG channels. PAF is measured at channel Pz. Values are Pearson's r with p -values in brackets. * Significant ($p < .05$) correlation or difference between correlations that survives FDR correction

observed, but this effect disappeared when controlling for baseline (resting state) activity. Similarly, the significant group difference in frontoparietal theta phase coherence disappeared when values were adjusted for baseline (resting state). Together, these findings suggest that NF1 is characterised by aberrant resting state oscillatory activity and highlight the importance of accounting for resting state (baseline) differences when drawing conclusions about task-related differences in oscillatory activity between groups.

Resting state power

Resting state delta and theta power were significantly higher in NF1 than in typically developing controls, in line with our hypothesis. Both of these significant group differences had large effect sizes. This finding is consistent with, and builds on, previous reports in the NF1 population [17] and in other neurodevelopmental disorders [37]. For instance, Ribeiro et al. [17] observed significantly higher theta power and a non-significant trend towards higher delta power in the NF1 cohort. Moreover, a review by Newson and Thiagarajan [37] of behaviourally relevant frequency bands during resting state EEG in psychiatric disorders, including ADHD, reported that one of the most dominant abnormalities is increased power in slower frequencies.

Although the mechanisms underlying abnormally high slow wave activity in NF1 are not understood [17], previous studies using animal models of disrupted myelination have demonstrated that loss of myelin is associated with an increase in slow wave theta power [59]. The well-documented white matter microstructure abnormalities and myelin deficits in NF1 [60, 61] could therefore account for the high slow wave resting state oscillatory activity observed in the current study. Dysregulation of the inhibitory neurotransmitter, gamma-aminobutyric acid (GABA) should also be considered as a mechanism underlying excessive resting state power. A handful of human studies report a GABA deficiency in children/adolescents with an NF1 diagnosis [18, 62]. Reduced inhibition as a result of a GABA deficiency might explain the excessive slow-wave (i.e. delta/theta) power observed.

Consistent with our prediction, direct tests of oscillatory power reactivity in the NF1 group showed that resting state power was significantly higher during eyes closed relative to eyes open in the delta, theta, and alpha bands, whilst the opposite pattern was observed in the gamma band. This demonstrates that resting state power reactivity follows the typical pattern observed in neurotypical populations [39] and builds on previous indirect suggestion (i.e. a non-significant group \times condition interaction) reported by Ribeiro et al. [17].

Finally, delta and theta power showed significant negative correlations with age in typically developing controls, consistent with existing literature showing that increasing age is associated with a reduction in slow wave resting state power throughout development [30, 32]. The same correlations were non-significant for NF1, though there were no significant differences in correlations between groups. However, the relatively small sample size limits our ability to draw definitive conclusions about whether the relationship between age and oscillatory power is atypical in NF1.

Peak alpha frequency

PAF was significantly lower in the NF1 group relative to typically developing controls, with a large effect size. This builds on a non-significant trend towards a lower PAF observed in one previous study in NF1 [17] and is consistent with investigations of PAF in other neurodevelopmental disorders [55, 63]. PAF is thought to reflect an index of cognitive preparedness [64], attentional processing [65], and memory ability [64, 66]. Despite this, we did not observe a significant correlation between PAF and working memory ability using performance on an auditory n-back task in either the control or NF1 group. However, again, the relatively small sample size was not optimal to address this, and it is possible that significant associations may be found with a larger sample.

We observed a positive age-PAF correlation in typically developing controls that was not present in NF1, and these correlations differed significantly between groups, suggesting that the relationship between PAF and age is disrupted in NF1. The age-PAF correlation in the control group is in accordance with existing literature in typically developing children, where increased PAF is observed throughout childhood, stabilising at ~ 10 Hz during late adolescence/early adulthood [67]. This increase in PAF is thought to index neural network maturation [68, 69] that facilitates improved and efficient connectivity [31, 32]. Moreover, the absence of a significant PAF-age correlation in the NF1 group is consistent with previous research in other neurodevelopmental disorders that has reported the absence of a relationship between PAF and age [56]. It has been suggested that in neurodevelopmental disorders in which overall cognitive function is disrupted and does not reliably map onto chronological age, PAF might instead be associated with Intelligence Quotient (IQ) [56]. Future studies measuring PAF (and other oscillatory measures) should consider including full-scale IQ testing using standardised measures and a non-NF1 developmentally delayed control group to disentangle generic effects of developmental delay and condition-specific effects.

Task-related power and coherence

Task-related (*unadjusted*) theta power was significantly higher in the NF1 group relative to typically developing controls, but this effect disappeared when controlling for baseline (resting state) activity. Likewise, the significant group difference in frontoparietal theta phase coherence (NF1 > CON) disappeared when values were adjusted for baseline (resting state). The absence of a group difference in task-specific power and theta phase coherence may suggest that the NF1 population have a generally high level of oscillatory activity, particularly in low frequencies, which might explain the absence of a difference in task-specific modulation. These findings are inconsistent with our hypothesis that predicted aberrant WM-related theta power and phase coherence relative to controls based on existing research in other neurodevelopmental disorders [29, 34–36]. However, this dissimilarity to observations in other neurodevelopmental disorders is not entirely surprising as, although neurodevelopmental disorders often exhibit overlapping cognitive impairments (i.e. strong clinical similarities), the underlying neurophysiology of these impairments is not always the same [14]. In sum, the current study suggests that task-related oscillatory activity might not be a useful EEG marker of working memory impairment in NF1. Instead, a better EEG marker of working memory impairment in NF1 might be the ERP P3b component, which has been found to differ in latency and topographic distribution in NF1 relative to typically developing controls [16].

Strengths, limitations, and future directions

This study has informed the characterisation of NF1 and potential targets (e.g. abnormally high slow wave power) for (non-) pharmacological interventions targeting NF1. However, this contribution must be considered in light of several limitations. Our sample size was comparable to existing neuroimaging studies using NF1 samples [13–15, 17, 18]. As noted in the ‘Participants’ section, we had 79% power to detect a large effect size on oscillatory measures. However, we were likely underpowered for the examination of associations between oscillatory features and age/cognitive measures. Future studies with larger sample sizes would help to draw more definitive conclusions regarding individual differences in oscillatory abnormalities in NF1.

A second limitation of this study is that, whilst we investigated group differences in single frequency bands, it may be beneficial to examine the relationships between different frequency bands during working memory performance to further understand the basis of working memory deficits in NF1. For instance, theta-gamma phase-amplitude coupling is a neural marker associated with working memory performance [22] and has

provided a neural marker of poor working memory in other clinical disorders (e.g. schizophrenia, Alzheimer’s disease, and mild cognitive impairment [70, 71]). Moreover, we must acknowledge the suggestion within the literature that the n-back task is not a pure measure of working memory [72], which in turn may play a role in the absence of a group difference in WM-related oscillatory activity. However, we carefully selected a time window thought to be dominated by maintenance activity in an attempt to capture working memory. Nonetheless, future studies using other measures believed to tap into working memory would be a useful addition to strengthen the conclusions drawn here.

Furthermore, a limitation of the analyses in this study relates to the challenges of investigating neurophysiological outcomes in clinical samples in which comorbidities are common. NF1 was treated as a homogenous group, despite a number of individuals having a comorbid diagnosis of ASD and/or ADHD. Individuals with comorbid NF1 and ADHD exhibit a more severe cognitive deficit than individuals with NF1 but without ADHD [73]. Ribeiro and colleagues [17] ran sensitivity analyses to determine whether the significant group differences observed remained after removing participants with comorbid ADHD. The pattern of results remained similar after excluding these participants. However, given dimensional nature of attentional difficulties (e.g. different subtypes of ADHD) and the likely underpowered nature of these analyses, future studies with larger sample sizes would permit stronger sensitivity analyses to facilitate an understanding of whether co-existing comorbidities result in different oscillatory features to what is reported here.

Finally, it is important to consider the developmental nature of our findings. Specifically, would findings have been different had the age range been different? We believe that we may have observed a different oscillatory expression if the sample had been younger—e.g. infants. This prediction stems from a consideration of the discrepancy between animal and human investigations of GABA activity in NF1. As discussed in the ‘Resting state power’ section, human studies report GABA deficiency in adolescents with NF1 [18, 62], which might explain the excessive resting state slow-wave power observed. However, in contrast to the GABA deficiency reported in human research [18, 62], animal research suggests that NF1 is characterised by increased GABA and therefore increased inhibition [13, 74]. Two suggestions have been proposed for these discrepant findings [75]. Specifically, the discrepancy may arise from a difference in *how* (e.g. GABA transmission in animals vs. GABA concentration measured using magnetic resonance imaging in humans) or *when*

(i.e. developmental compensation) GABA is measured [75]. To develop understanding of the excessive slow-wave power observed in adolescents with NF1, future research could investigate resting state power during infancy. If slow-wave power is lower (relative to typically developing controls) in infancy as a result of increased GABA (as shown in animal studies), this would suggest that excessive slow-wave power during adolescence is a result of homeostatic compensation to excessive inhibition during early life [76].

A recent study by Carter-Leno and colleagues [75] provides increased weight in support of a hypothesised lower slow-wave power in infancy. They demonstrated increased resting state inhibition relative to excitation (i.e. excitation/inhibition (E/I) imbalance) in 10-month-old infants with NF1, in line with increased inhibition reported in animals. As a next step, researchers could investigate E/I balance in adolescents with NF1 (using novel methods like FOOOF [77]) to further investigate the existence of homeostatic compensation mechanisms in this population. If increased excitation relative to inhibition is observed in adolescents (i.e. the opposite of that reported during infancy), this might indicate homeostatic compensation to excessive inhibition during early life [76]. Collectively, these two recommendations for future research would not only advance understanding of excessive resting state slow-wave power in adolescents with NF1 but also shed light on the developmental trajectory of oscillatory activity and the discrepant animal and human research surrounding GABA in this population.

Conclusions

This study investigated oscillatory activity both at rest and during the performance of a working memory task. We found that adolescents with NF1 display aberrant oscillatory activity relative to typically developing controls during rest. Specifically, NF1 is characterised by excessive resting state oscillatory activity, particularly at lower frequencies, and a lower peak alpha frequency. Moreover, we found that apparent group differences in working memory task-related oscillatory power and frontoparietal coherence disappeared when accounting for baseline levels from resting state. These findings provide insights that can inform the characterisation of NF1, as well as the design of (non-) pharmacological interventions targeting NF1, and also highlight important avenues for future research.

Abbreviations

ADHD	Attention-deficit hyperactivity disorder
ASD	Autism spectrum disorder
CON	Control

TDCS	Transcranial direct current stimulation
EEG	Electroencephalography
ERP	Event-Related Potential
fMRI	Functional Magnetic Resonance Imaging
GABA	Gamma-aminobutyric acid
ICA	Independent Components Analysis
IQ	Intelligence Quotient
ISPC	Inter-site phase clustering
M	Mean
ML	Mid-frontal-left-parietal
MM	Mid-frontal-mid-parietal
MR	Mid-frontal-right-parietal
NF1	Neurofibromatosis Type 1
PAF	Peak alpha frequency
SD	Standard deviation
VABS-II	Vineland Adaptive Behaviour Scale
Vineland ABC	Vineland Adaptive Behaviour Composite

Supplementary Information

The online version contains supplementary material available at <https://doi.org/10.1186/s11689-023-09492-y>.

Additional file 1: Sub-sample demographic and behavioural information. **Table 1.** Descriptive and inferential statistics for age, sex, Vineland ABC scores, and auditory n-back performance. **Table 2.** Descriptive and inferential statistics for EEG visual n-back task performance (hits % – false alarms %).

Additional file 2: Statistical analysis of task-related *unadjusted* power and theta coherence. **Table 1.** Power (*unadjusted*): descriptive and inferential statistics. **Table 2.** Theta phase coherence (*unadjusted*): descriptive and inferential statistics.

Additional file 3: Resting state analyses for mid-frontal theta power and theta phase coherence. **Table 1.** Resting state (eyes open) mid-frontal theta power: descriptive and inferential statistics. **Table 2.** Resting state (eyes open) theta phase coherence: descriptive and inferential statistics.

Additional file 4: Scatterplots. **Fig. 1.** Scatterplots between EEG measures and age. **Fig. 2.** Scatterplots between EEG measures and Vineland ABC scores. **Fig. 3.** Scatterplots between EEG measures and auditory n-back performance (working memory).

Additional file 5: Sensitivity Analyses. **Table 1.** Sensitivity analyses outcomes.

Acknowledgements

We would like to thank the participants and their families for their participation, and Emily Pye, JeYoung Jung, and Hemavathy Ramalingham for their roles in data collection.

Authors' contributions

SB, SG, JG, GP, and JT conceptualised and designed the study. SG was responsible for participant recruitment. SG, GP, and JT were responsible for data collection. SB analysed the data and wrote the original manuscript draft. SB, SG, LB, GP, and JT contributed towards interpretation of the data. All authors contributed towards reviewing and editing the manuscript. All authors read and approved the final manuscript.

Funding

Data collection was funded by the Newlife Charity for Disabled Children. The analysis and write-up was conducted as part of a PhD funded by the Economic and Social Research Council (ESRC), awarded to Samantha Booth (grant number ES/P000665/1). The funders had no role in the study design, data collection, data analysis, statistical analysis, interpretation of the data, writing of the paper, or decision regarding when to submit the publication.

Availability of data and materials

The datasets used and/or analysed during the current study are available from the corresponding author on reasonable request.

Declarations

Ethics approval and consent to participate

This study received ethical approval from the Greater Manchester West Research Ethics Committee (17/NW/0364) and was conducted in accordance with the Declaration of Helsinki. Parents/guardians gave oral and written consent, and adolescents assent (where developmentally appropriate), prior to participation.

Consent for publication

Not applicable.

Competing interests

The authors declare that they have no competing interests.

Received: 25 August 2022 Accepted: 30 June 2023

Published online: 22 August 2023

References

- Evans DG, Howard E, Giblin C, Clancy T, Spencer H, Huson SM, Laloo F. Birth incidence and prevalence of tumor-prone syndromes: estimates from a UK family genetic register service. *Am J Med Genet A*. 2010;152(2):327–32.
- Gutmann DH, Ferner RE, Listerick RH, Korf BR, Wolters PL, Johnson KJ. Neurofibromatosis type 1. *Nat Rev Dis Primers*. 2017;3(1):1–7.
- Garg S, Lehtonen A, Huson SM, Emsley R, Trump D, Evans DG, Green J. Autism and other psychiatric comorbidity in neurofibromatosis type 1: evidence from a population-based study. *Dev Med Child Neurol*. 2013;55(2):139–45.
- Beaussart ML, Barbarot S, Mauger C, Roy A. Systematic review and meta-analysis of executive functions in preschool and school-age children with neurofibromatosis type 1. *J Int Neuropsychol Soc*. 2018;24(9):977–94.
- Crow AJD, Janssen JM, Marshall C, Moffit A, Brennan L, Kohler CG, Roalf DR, Moberg PJ. A systematic review and meta-analysis of intellectual, neuropsychological, and psychoeducational functioning in neurofibromatosis type 1. *Am J Med Genet Part A*. 2022;188A:2277–92. <https://onlinelibrary-wiley-com.manchester.idm.oclc.org/action/showCitForMats?doi=10.1002%2Fajmg.a.62773>.
- Hyman SL, Shores A, North KN. The nature and frequency of cognitive deficits in children with neurofibromatosis type 1. *Neurology*. 2005;65(7):1037–44.
- Baudou E, Nemmi F, Biotteau M, Maziero S, Peran P, Chaix Y. Can the cognitive phenotype in neurofibromatosis type 1 (NF1) be explained by neuroimaging? A review. *Front Neurol*. 2020;10:1373.
- Krawinkel LA, Engel AK, Hummel FC. Modulating pathological oscillations by rhythmic non-invasive brain stimulation—a therapeutic concept? *Front Syst Neurosci*. 2015;9:33.
- Heinrich H, Busch K, Studer P, Erbe K, Moll GH, Kratz O. EEG spectral analysis of attention in ADHD: implications for neurofeedback training? *Front Hum Neurosci*. 2014;8:611.
- Reinhart RM, Nguyen JA. Working memory revived in older adults by synchronizing rhythmic brain circuits. *Nat Neurosci*. 2019;22(5):820–7.
- Loitfelder M, Huijbregts SC, Veer IM, Swaab HS, Van Buchem MA, Schmidt R, Rombouts SA. Functional connectivity changes and executive and social problems in neurofibromatosis type I. *Brain Connectivity*. 2015;5(5):312–20.
- Ibrahim AF, Montojo CA, Haut KM, Karlsgodt KH, Hansen L, Congdon E, Rosser T, Bilder RM, Silva AJ, Bearden CE. Spatial working memory in neurofibromatosis 1: Altered neural activity and functional connectivity. *NeuroImage: Clin*. 2017;15:801–11.
- Shilyansky C, Karlsgodt KH, Cummings DM, Sidiropoulou K, Hardt M, James AS, Ehninger D, Bearden CE, Poirazi P, Jentsch JD, Cannon TD. Neurofibromin regulates corticostriatal inhibitory networks during working memory performance. *Proc Natl Acad Sci*. 2010;107(29):13141–6.
- Bluschke A, von der Hagen M, Papenhagen K, Roessner V, Beste C. Response inhibition in attention deficit disorder and neurofibromatosis type 1—clinically similar, neurophysiologically different. *Sci Rep*. 2017;7(1):1–8.
- Bluschke A, von der Hagen M, Papenhagen K, Roessner V, Beste C. Conflict processing in juvenile patients with neurofibromatosis type 1 (NF1) and healthy controls—Two pathways to success. *NeuroImage: Clin*. 2017;14:499–505.
- Pobric G, Taylor JR, Ramalingam HM, Pye E, Robinson L, Vassallo G, Jung J, Bhandary M, Szumanska-Ryt K, Theodosiou L, Evans DG. Cognitive and electrophysiological correlates of working memory impairments in neurofibromatosis type 1. *J Autism Dev Disord*. 2022;52(4):1478–94.
- Ribeiro MJ, d'Almeida OC, Ramos F, Saraiva J, Silva ED, Castelo-Branco M. Abnormal late visual responses and alpha oscillations in neurofibromatosis type 1: a link to visual and attention deficits. *J Neurodev Disord*. 2014;6(1):1–9.
- Ribeiro MJ, Violante IR, Bernardino I, Edden RA, Castelo-Branco M. Abnormal relationship between GABA, neurophysiology and impulsive behavior in neurofibromatosis type 1. *Cortex*. 2015;64:194–208.
- Bastiaansen M, Mazaheri A, Jensen O. Beyond ERPs. In: *The Oxford Handbook of Event-Related Potential Components*. 2011.
- Cohen MX. Analyzing neural time series data: theory and practice. Cambridge: MIT press; 2014. <https://doi.org/10.7551/mitpress/9609.001.0001>.
- Albouy P, Martinez-Moreno ZE, Hoyer RS, Zatorre RJ, Baillet S. Supramodality of neural entrainment: Rhythmic visual stimulation causally enhances auditory working memory performance. *Sci Adv*. 2022;8(8):eabj9782.
- Lisman JE, Jensen O. The theta-gamma neural code. *Neuron*. 2013;77(6):1002–16.
- Roux F, Uhlhaas PJ. Working memory and neural oscillations: alpha-gamma versus theta-gamma codes for distinct WM information? *Trends Cogn Sci*. 2014;18(1):16–25.
- Fell J, Axmacher N. The role of phase synchronisation in memory processes. *Nat Rev Neurosci*. 2011;12(2):105–18.
- Daume J, Gruber T, Engel AK, Fries U. Phase-amplitude coupling and long-range phase synchronization reveal frontotemporal interactions during visual working memory. *J Neurosci*. 2017;37(2):313–22.
- Sarthein J, Petsche H, Rappelsberger P, Shaw GL, Von Stein A. Synchronization between prefrontal and posterior association cortex during human working memory. *Proc Natl Acad Sci*. 1998;95(12):7092–6.
- Meyer M, Endedijk HM, Van Ede F, Hunnius S. Theta oscillations in 4-year-olds are sensitive to task engagement and task demands. *Sci Rep*. 2019;9(1):1–1.
- Michels L, Luchinger R, Koenig T, Martin E, Brandeis D. Developmental changes of BOLD signal correlations with global human EEG power and synchronization during working memory. *PLoS ONE*. 2012;7(7): e39447.
- Missonnier P, Hasler R, Perroud N, Herrmann FR, Millet P, Richiardi J, Malafosse A, Giannakopoulos P, Baud P. EEG anomalies in adult ADHD subjects performing a working memory task. *Neuroscience*. 2013;241:135–46.
- Gmehl D, Thomas C, Weisbrod M, Walther S, Pfüller U, Resch F, Oelkers-Ax R. Individual analysis of EEG background-activity within school age: impact of age and sex within a longitudinal data set. *Int J Dev Neurosci*. 2011;29(2):163–70.
- Rodriguez-Martinez EI, Barriga-Paulino CI, Rojas-Benjumea MA, Gómez CM. Spontaneous theta rhythm and working memory co-variation during child development. *Neurosci Lett*. 2013;550:134–8.
- Segalowitz SJ, Santesso DL, Jetha MK. Electrophysiological changes during adolescence: a review. *Brain Cogn*. 2010;72(1):86–100.
- Lenartowicz A, Delorme A, Walshaw PD, Cho AL, Bilder RM, McGough JJ, McCracken JT, Makeig S, Loo SK. Electroencephalography correlates of spatial working memory deficits in attention-deficit/hyperactivity disorder: vigilance, encoding, and maintenance. *J Neurosci*. 2014;34(4):1171–82.
- Martínez-Briones BJ, Fernández-Harmony T, Garófalo Gómez N, Biscay-Lirio RJ, Bosch-Bayard J. Working memory in children with learning disorders: An EEG power spectrum analysis. *Brain Sci*. 2020;10(11):817.
- Jang KM, Kim MS, Kim DW. The dynamic properties of a brain network during spatial working memory tasks in college students with ADHD traits. *Front Hum Neurosci*. 2020;14: 580813.
- Yuk V, Urbain C, Anagnostou E, Taylor MJ. Frontoparietal network connectivity during an n-back task in adults with autism spectrum disorder. *Front Psych*. 2020;11: 551808.
- Newson JJ, Thiagarajan TC. EEG frequency bands in psychiatric disorders: a review of resting state studies. *Front Human Neurosci*. 2018;12:521.

38. Silva G, Ribeiro MJ, Costa GN, Violante I, Ramos F, Saraiva J, Castelo-Branco M. Peripheral attentional targets under covert attention lead to paradoxically enhanced alpha desynchronization in neurofibromatosis type 1. *PLoS ONE*. 2016;11(2): e0148600.
39. Geller AS, Burke JF, Sperling MR, Sharan AD, Litt B, Baltuch GH, Lucas TH II, Kahana MJ. Eye closure causes widespread low-frequency power increase and focal gamma attenuation in the human electrocorticogram. *Clin Neurophysiol*. 2014;125(9):1764–73.
40. Rawley JB, Constantinidis C. Neural correlates of learning and working memory in the primate posterior parietal cortex. *Neurobiol Learn Mem*. 2009;91(2):129–38.
41. Kane MJ, Engle RW. The role of prefrontal cortex in working-memory capacity, executive attention, and general fluid intelligence: an individual-differences perspective. *Psychon Bull Rev*. 2002;9(4):637–71.
42. G*Power. <http://www.gpower.hhu.de/>. Accessed 16 Aug 2022.
43. Neurofibromatosis NI. Conference statement. National Institutes of Health Consensus Development Conference. *Arch Neurol*. 1988;45(5):575–8.
44. Hill TL, Saulnier, CA, Cicchetti D, Gray SAO, Carter AS, Vineland III. In: *Encyclopaedia of autism spectrum disorders*. New York: Springer New York; 2017. p. 1–4.
45. Jensen O, Tesche CD. Frontal theta activity in humans increases with memory load in a working memory task. *Eur J Neurosci*. 2002;15(8):1395–9.
46. Taylor, JR. Github. <https://www.github.com/jason-taylor>. Accessed 16 Aug 2022.
47. Cohen, MX. Tutorial neural time series analysis. https://github.com/AndreIZn/Tutorial_neural_time_series_analysis. Accessed 16 Aug 2022.
48. Gudi-Mindermann H, Rimmele JM, Nolte G, Bruns P, Engel AK, Röder B. Working memory training in congenitally blind individuals results in an integration of occipital cortex in functional networks. *Behav Brain Res*. 2018;348:31–41.
49. Wang J, Barstein J, Ethridge LE, Mosconi MW, Takarae Y, Sweeney JA. Resting state EEG abnormalities in autism spectrum disorders. *J Neurodev Disord*. 2013;5(1):1–4.
50. Valipour S, Shaligram AD, Kulkarni GR. Detection of an alpha rhythm of EEG signal based on EEGLAB. *Int J Eng Res Appl*. 2014;4(1):154–9.
51. Voss, R. P. 'f/noise' In music and speech. <https://escholarship.org/content/qt04t64495/qt04t64495.pdf>. 1975. Accessed 16 Aug 2022.
52. Cohen, MX. Laplacian Perrin. https://github.com/mikexcohen/AnalyzingNeuralTimeSeries/blob/main/laplacian_perrinX.m. Accessed 16 Aug 2022.
53. Srinivasan R, Winter WR, Ding J, Nunez PL. EEG and MEG coherence: measures of functional connectivity at distinct spatial scales of neocortical dynamics. *J Neurosci Methods*. 2007;166(1):41–52.
54. Anguera JA, Boccanfuso J, Rintoul JL, Al-Hashimi O, Faraji F, Janowich J, Kong E, Larraburo Y, Rolfe C, Johnston E, Gazzaley A. Video game training enhances cognitive control in older adults. *Nature*. 2013;501(7465):97.
55. Pritchard WS. The brain in fractal time: 1/f-like power spectrum scaling of the human electroencephalogram. *Int J Neurosci*. 1992;66(1–2):119–29.
56. Dickinson A, DiStefano C, Senturk D, Jeste SS. Peak alpha frequency is a neural marker of cognitive function across the autism spectrum. *Eur J Neurosci*. 2018;47(6):643–51.
57. Levine TM, Materok A, Abel J, O'Donnell M, Cutting LE. Cognitive profile of neurofibromatosis type 1. *Semin Pediatr Neurol*. 2006;13(1):8–20. <https://doi.org/10.1016/j.spen.2006.01.006>.
58. Benjamini Y, Hochberg Y. Controlling the false discovery rate: a practical and powerful approach to multiple testing. *J Roy Stat Soc: Ser B (Methodol)*. 1995;57(1):289–300.
59. Dubey M, Pascual-García M, Helmes K, Wever DD, Hamada MS, Kushner SA, Kole MH. Myelination synchronizes cortical oscillations by consolidating parvalbumin-mediated phasic inhibition. *Elife*. 2022;11:e73827. <https://elifesciences.org/articles/73827>.
60. Asleh J, Shofty B, Cohen N, Kavushansky A, López-Juárez A, Constantini S, Ratner N, Kahn I. Brain-wide structural and functional disruption in mice with oligodendrocyte-specific NF1 deletion is rescued by inhibition of nitric oxide synthase. *Proc Natl Acad Sci*. 2020;117(36):22506–13.
61. Karlsgodt KH, Rosser T, Lutkenhoff ES, Cannon TD, Silva A, Bearden CE. Alterations in white matter microstructure in neurofibromatosis-1. *PLoS ONE*. 2012;7(10):e47854. <https://doi.org/10.1371/journal.pone.0047854>, <https://journals.plos.org/plosone/article?id=10.1371/journal.pone.0047854>.
62. Violante IR, Ribeiro MJ, Edden RA, Guimarães P, Bernardino I, Rebola J, Cunha G, Silva E, Castelo-Branco M. GABA deficit in the visual cortex of patients with neurofibromatosis type 1: genotype–phenotype correlations and functional impact. *Brain*. 2013;136(3):918–25.
63. Lansbergen MM, Arns M, van Dongen-Boomsma M, Spronk D, Buitelaar JK. The increase in theta/beta ratio on resting-state EEG in boys with attention-deficit/hyperactivity disorder is mediated by slow alpha peak frequency. *Prog Neuropsychopharmacol Biol Psychiatry*. 2011;35(1):47–52.
64. Angelakis E, Lubar JF, Stathopoulou S, Kounios J. Peak alpha frequency: an electroencephalographic measure of cognitive preparedness. *Clin Neurophysiol*. 2004;115(4):887–97.
65. Zhang Y, Lu Y, Wang D, Zhou C, Xu C. Relationship between individual alpha peak frequency and attentional performance in a multiple object tracking task among ice-hockey players. *PLoS ONE*. 2021;16(5): e0251443.
66. Klimesch W, Schimke HA, Pfurtscheller G. Alpha frequency, cognitive load and memory performance. *Brain Topogr*. 1993;5(3):241–51.
67. Marcuse LV, Schneider M, Mortati KA, Donnelly KM, Arnedo V, Grant AC. Quantitative analysis of the EEG posterior-dominant rhythm in healthy adolescents. *Clin Neurophysiol*. 2008;119(8):1778–81.
68. Klimesch W, Sauseng P, Hanslmayr S. EEG alpha oscillations: the inhibition–timing hypothesis. *Brain Res Rev*. 2007;53(1):63–88.
69. Valdés-Hernández PA, Ojeda-González A, Martínez-Montes E, Lage-Castellanos A, Virués-Alba T, Valdés-Urrutia L, Valdes-Sosa PA. White matter architecture rather than cortical surface area correlates with the EEG alpha rhythm. *Neuroimage*. 2010;49(3):2328–39.
70. Barr MS, Rajji TK, Zomorodi R, Radhu N, George TP, Blumberger DM, Daskalakis ZJ. Impaired theta-gamma coupling during working memory performance in schizophrenia. *Schizophr Res*. 2017;189:104–10.
71. Goodman MS, Kumar S, Zomorodi R, Ghazala Z, Cheam AS, Barr MS, Daskalakis ZJ, Blumberger DM, Fischer C, Flint A, Mah L. Theta-gamma coupling and working memory in Alzheimer's dementia and mild cognitive impairment. *Front Aging Neurosci*. 2018;10:101.
72. Miller KM, Price CC, Okun MS, Montijo H, Bowers D. Is the n-back task a valid neuropsychological measure for assessing working memory? *Arch Clin Neuropsychol*. 2009;24(7):711–7.
73. Lidzba K, Granström S, Lindenau J, Mautner VF. The adverse influence of attention-deficit disorder with or without hyperactivity on cognition in neurofibromatosis type 1. *Dev Med Child Neurol*. 2012;54(10):892–7.
74. Cui Y, Costa RM, Murphy GG, Elgersma Y, Zhu Y, Gutmann DH, Parada LF, Mody I, Silva AJ. Neurofibromin regulation of ERK signaling modulates GABA release and learning. *Cell*. 2008;135(3):549–60.
75. Carter Leno V, Begum-Ali J, Goodwin A, Mason L, Pasco G, Pickles A, Garg S, Green J, Charman T, Johnson MH, Jones EJ. Infant excitation/inhibition balance interacts with executive attention to predict autistic traits in childhood. *Mol Autism*. 2022;13(1):1–3.
76. Nelson SB, Valakh V. Excitatory/inhibitory balance and circuit homeostasis in autism spectrum disorders. *Neuron*. 2015;87(4):684–98.
77. Donoghue T, Haller M, Peterson EJ, Varma P, Sebastian P, Gao R, Noto T, Lara AH, Wallis JD, Knight RT, Shetyuk A. Parameterizing neural power spectra into periodic and aperiodic components. *Nat Neurosci*. 2020;23(12):1655–65.
78. Montefusco-Siegmund R, Maldonado PE, Devia C. Effects of ocular artifact removal through ICA decomposition on EEG phase. In 2013 6th International IEEE/EMBS Conference on Neural Engineering (NER). San Diego: IEEE. 2013; pp.1374–1377.

Publisher's Note

Springer Nature remains neutral with regard to jurisdictional claims in published maps and institutional affiliations.